ELSEVIER

Journal of Alloys and Compounds 293–295 (1999) 202–212

Journal of ALLOYS AND COMPOUNDS

Chemical structure and bonding characteristics of metal hydrogen systems studied by the surface analytical techniques SIMS and XPS

H. Züchner*, J. Kintrup, R. Dobrileit, I. Untiedt

Institute of Physical Chemistry, University of Münster, Schloßplatz 4+7, D-48149 Münster, Germany

Abstract

Secondary ion mass spectrometry (SIMS) as well as photoelectron spectroscopy (XPS) are powerful tools for studying special properties of metal hydrogen systems and the interaction of hydrogen and metals. SIMS experiments have now also been extended to transition metal hydrogen systems with small hydrogen solubilities by using intelligent mass spectra accumulation. As known from studies on other metal hydrogen systems (V–H, Nb–H etc.) the cluster ion Me_2H^+ is particularly characteristic for transition metal hydrogen systems. In AB_5-type alloy hydrogen systems a quite different behavior is observed. We have focussed our attention on studying the properties of the $LaNi_5$-alloy with nickel partially substituted by Al or Ag. The mass spectra, especially the negative ones, show a strong Ni–H, a weaker Ag–H and almost no Al–H bond, which explains the decrease in hydrogen storage capacity when going from pure $LaNi_5$ to $LaNi_{5-X}Ag_X$ and $LaNi_{5-X}Al_X$. Pressure–concentration like isotherms are obtained for the $LaNi_{5-X}Al_XD_Y$ system by SIMS with highest spectral purity when applying a synchronous in situ gasvolumetric hydrogen charging procedure during the SIMS analysis under Ar^+ ion bombardment. XPS studies on metal hydrogen systems yield valuable information concerning chemical and physical properties, which are complementary to the SIMS results. A hydrogen induced chemical shift and changes in the line shape of the valence band and the core electron levels are observed in $LaNi_5H_Y$ photoelectron spectra if H_2^+ ion implantation is used as an alternative hydrogen charging technique. The XPS results indicate the existence of a Ni–H bond in excellent agreement with the SIMS measurements.

Keywords: Chemical structure; Bonding characteristics; SIMS; XPS; Hydrogen storage intermetallics

1. Introduction

Although AB_5-type multi-component alloys are nowadays widely used as electrode materials in NiMH batteries, there is still a lack of knowledge on the electronic structure and chemical bonding characteristics of these materials. Such knowledge is required to improve or develop new hydrogen storage materials effectively.

Surface analytical techniques offer new possibilities to study not only the surface but also the bulk behavior of such metal hydrogen systems. Among these techniques are secondary ion mass spectrometry (SIMS) and secondary neutral particle mass spectrometry (SNMS) which both permit the direct detection of hydrogen with high sensitivity. They allow the analysis of elemental surface composition. They also yield information about the chemical structure and the hydrogen bonds by analysis of the polarity and the composition of hydrogen containing cluster ions, which are emitted in the same form as they occur in the solid sample [1].

X-ray photoelectron spectroscopy (XPS) complements SIMS measurements in an ideal fashion, even though hydrogen and the hydrogen influence can only be detected indirectly via the chemical shift in the electron energies of the metal atoms and via line shape changes [2]. The experimental photoelectron valence band spectra can be compared with band structure calculations. Spectral analysis thus gives information about the metal hydrogen bond.

In contrast to other authors (e.g. [3–7]) who apply surface analytical techniques to examine the activation and passivation of hydrogen storage materials we focus our attention in this paper on bulk properties, that means on electronic and chemical structures which are also detectable by SIMS and XPS.

Application of these surface analytical techniques requires ultra high vacuum conditions ($p<10^{-7}$ Pa), clean sample surfaces and a – for the respective technique – sufficiently high hydrogen concentration in the surface region. Loss of hydrogen from the sample due to vacuum

*Corresponding author.

0925-8388/99/$ – see front matter
PII: S0925-8388(99)00420-X

conditions or surface contamination by elements like oxygen, carbon or nitrogen has to be avoided.

2. Experimental

2.1. Sample preparation

An overview of the specially prepared samples and the applied hydrogen (deuterium) charging methods and conditions is given in Table 1. All elemental samples were obtained from commercial manufacturers (Aldrich, Goodfellow, Johnson Mathey). The alloys were synthesized by the group of Prof. L. Schlapbach from the university of Fribourg (polycrystalline $LaNi_{5-X}Al_X$ samples), Forschungszentrum Jülich ($LaNi_5$ single crystal) and ourselves. All samples were abrased with SiC emery paper, polished with diamond paste and cleaned in an ultrasonic bath containing acetone and methanol.

2.2. SIMS

Measurements were carried out in a combined SIMS/AES-instrument (Balzers/Physical Electronics) described in detail in [8]. The base pressure of the whole system is below $4\cdot10^{-8}$ Pa. Mass spectra were taken with a step width of 1/16 AMU. The original ion gun (Balzers PIQ 102, energy 3 keV, current density $2\cdot10^{-6}$ A/cm^2) was used for SIMS analysis of the transition metal hydrogen systems, for Ar^+ sputter cleaning of the samples and for D_2^+ (H_2^+) implantation – by switching the operating gas from argon to deuterium – as well. For reasons of proper comparison all metals have been investigated applying identical measuring conditions.

For the alloys a differentially pumped ion gun (Specs IQE12/38) was used instead of the original gun. Ar^+ ions of 5 keV energy at current densities in the 10^{-6} to 10^{-5} A/cm^2 range were used for the measurements. Deuterium for in situ charging during the SIMS analysis can be admitted to the analysis chamber through a separate leak valve up to pressures of $\approx5\cdot10^{-3}$ Pa. Due to the differential pumping of the ion gun the Ar^+ ion formation is independent of the deuterium inlet [19].

Secondary ion intensities of pure transition metals are often rather low (<10 counts/s in some cases) with bad signal/noise ratios. Therefore, intelligent mass spectra accumulation was used for spectra acquisition, as described in [12]. An example of the improvement in sensitivity by accumulation of spectra is given in Fig. 1.

Generally, the hydrogen concentration in the samples prepared by ion implantation is practically unknown, as hydrogen atoms in the surface area may be lost either by diffusion into the bulk or by desorption processes. Nevertheless, due to the ion bombardment in the SIMS experiment [1] the hydrogen concentration in the surface region, investigated by SIMS, is mostly independent of the deuterium charging method. The ion bombardment leads to an expanded metal lattice and thus to a hydrogen rich surface phase, even at small bulk concentrations.

2.3. XPS

The instrument used is an ESCA3 spectrometer (Vacuum Generators) with a modified vacuum system [9] that achieves a base pressure of approximately $5\cdot10^{-7}$ Pa. The non-monochromatic aluminum X-ray source (1486.6 eV) is operated at a maximum power of 240 W (20 mA at 12 kV). The concentric hemisphere analyser is operated in constant analyser energy (CAE) mode with a pass energy of 50 eV resulting in a resolution of 1.50 eV measured as FWHM of the Ag $3d_{5/2}$ line. The spectrometer was calibrated using the binding energies of copper[1]. A Penning-type ion gun (Vacuum Generators AG 2) was used for sample cleaning (3 keV Ar^+) and hydrogen implantation (8 keV H_2^+). Photoelectron spectra were acquired with 0.1 eV step width. A Shirley-type background [11] was subtracted from the detail spectra.

[1] E_B (Cu 3p)=75.14 eV, E_B (Cu L_3MM)=567.96 eV, E_B (Cu $2p_{3/2}$)=932.67 eV [10].

Table 1
Samples and applied hydrogen charging methods

Sample	Analysis method	Hydrogen (deuterium) charging method	Charging conditions
$LaNi_5$	XPS	H_2^+ ion implantation (8 keV) under sample cooling ($N_{2,liquid}$)	ion dose= $2\cdot10^{18}$ H atoms/cm^2
$LaNi_5$	SIMS	in situ during SIMS analysis	$p(D_2)_{max}=4.3\cdot10^{-3}$ Pa
$LaNi_{5-X}Al_X$ (X=0.7, 0.85, 1)	SIMS	in situ during SIMS analysis	$p(D_2)_{max}=4.3\cdot10^{-3}$ Pa
$LaNi_{4.5}Ag_{0.5}$	SIMS	in situ during SIMS analysis	$p(D_2)_{max}=2\cdot10^{-3}$ Pa
La, Ti, V	SIMS	gasvolumetrically before SIMS analysis	$p(D_2)=1\cdot10^5$ Pa
Cr, Mn, Fe, Co, Ni	SIMS	D_2^+ (H_2^+) ion implantation (3 keV)	ion dose= $1\cdot10^{17}$ D (H) atoms/cm^2

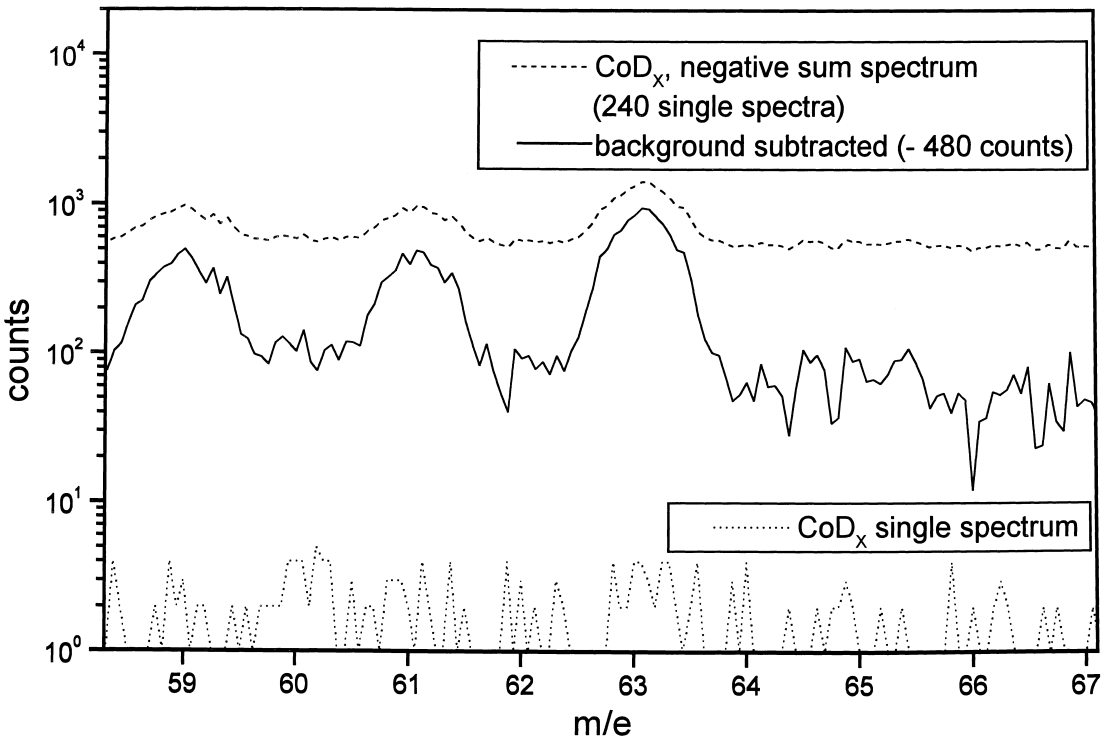

Fig. 1. Negative secondary ion spectra of CoD_x (intelligent mass spectra accumulation).

3. Results

3.1. SIMS

3.1.1. Transition metals

From all positive and negative metal–deuterium cluster ions the $Me_2D_X^+$ ($Me_2H_X^+$) ions emerged as the strongest and most deuterium-specific ones with the highest dynamic detection range. This is clearly demonstrated by a comparison of the emission of $Me_2D_X^+$ ($Me_2H_X^+$) secondary ions and deuterium (hydrogen) free Me_2^+ ions as shown in Fig. 2. This behavior and also the negligible intensity of MeD^+ ions compared to the Me^+ signal (not illustrated in this paper, see [12]) is typical of the first row of transition metal hydrogen systems[2].

The Me_2D^+ intensity increases from titanium to vanadium and chromium. For manganese with a half-filled 3d shell a steep drop occurs in the Me_2D^+ intensity, which then increases again progressively with the increase in the ordinary element number via iron, cobalt to nickel. $Me_2D_2^+$ signals appear only for titanium and vanadium. These are the two elements of the investigated samples that form stable dihydrides under normal conditions.

The emission intensity of the $Me_2D(H)^+$-ions and more so the intensity ratio, $Me_2D(H)^+/Me_2^+$, is an appropriate measure for the metal–hydrogen interaction and it reflects trends across the periodic table of the elements.

3.1.2. AB_5-type alloys

3.1.2.1. $LaNi_5D_X$ system

Fig. 3 shows the positive secondary ion mass spectrum of a sputter-cleaned $LaNi_5$ single crystal, which is charged gasvolumetrically in situ with Deuterium[3] *during* the SIMS analysis. The high $I(La^+)/I(LaO^+)$ intensity ratio and the existence of cluster ions containing more than two atoms (e.g. $La_2Ni_2^+$) indicate an extremely high sample (and spectrum) purity, which is superior to a polycrystalline sample charged electrochemically (spectra in [13]). The metal–deuterium cluster ions with the highest intensities are $LaNiD^+$, LaD^+, La_2NiD^+, La_2D^+ and $La_2Ni_2D^+$. With the exception of the small Ni_2D^+ peak deuterium always appears together with lanthanum in the positive mass spectrum. The intensity of the deuterium containing ions, however, is smaller than the intensity of the corresponding deuterium free ions (e.g. $I(LaNiD^+)$/

[2] We did not succeed to obtain any $Me_mD_n^{\pm}$ signal for zinc and copper even when ion implantation had been used for hydrogen charging. The hydrogen solubility is obviously too small in these two elements to detect metal hydrogen cluster ions by SIMS.

[3] Deuterium is used instead of hydrogen to separate the deuterium charging process from the influence of hydrogen in the residual gas.

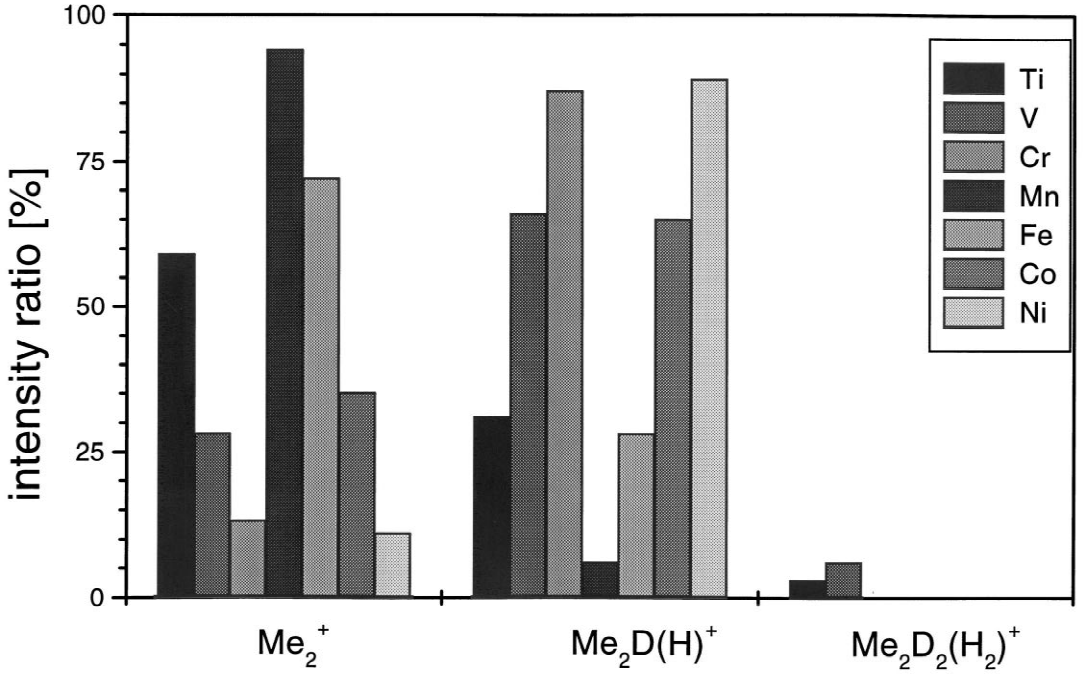

Fig. 2. Relative intensities of $Me_2D_X^+$ ($Me_2H_X^+$) cluster ions (sum of the cluster ions=100% for each element).

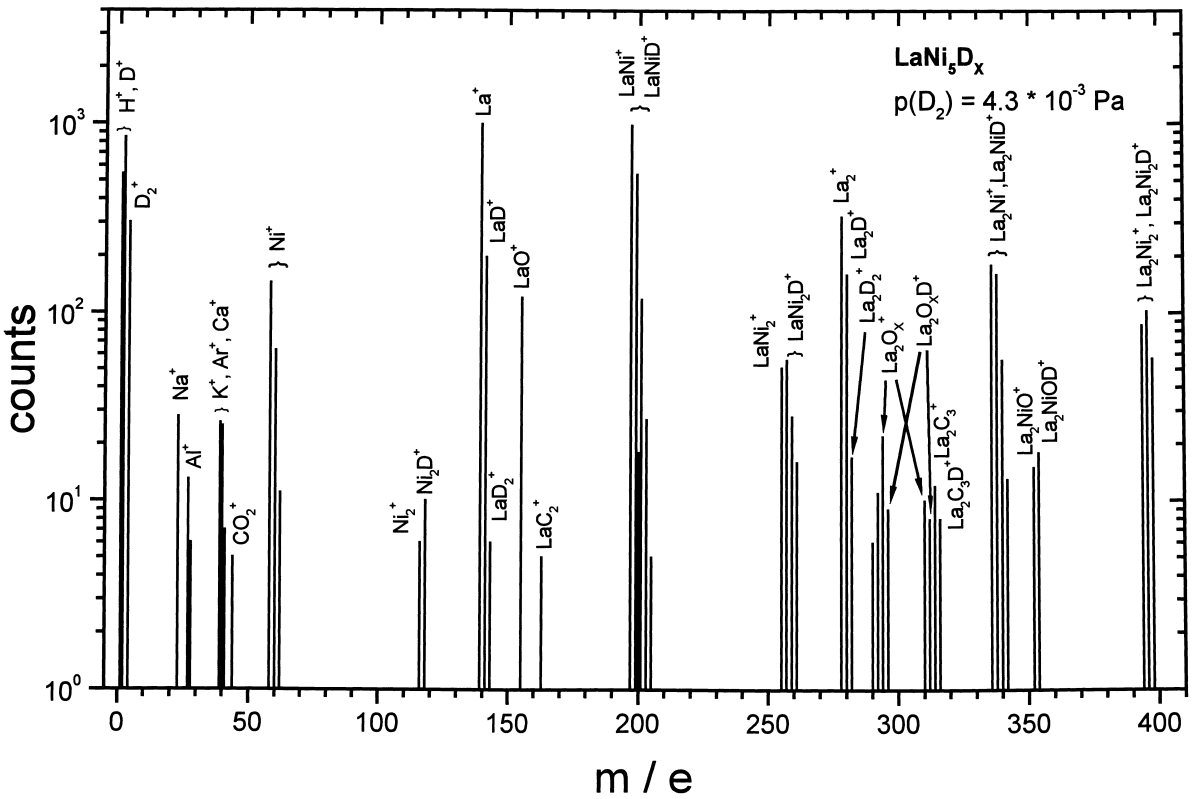

Fig. 3. Positive secondary ion mass spectrum of a $LaNi_5$ single crystal charged in situ with D_2.

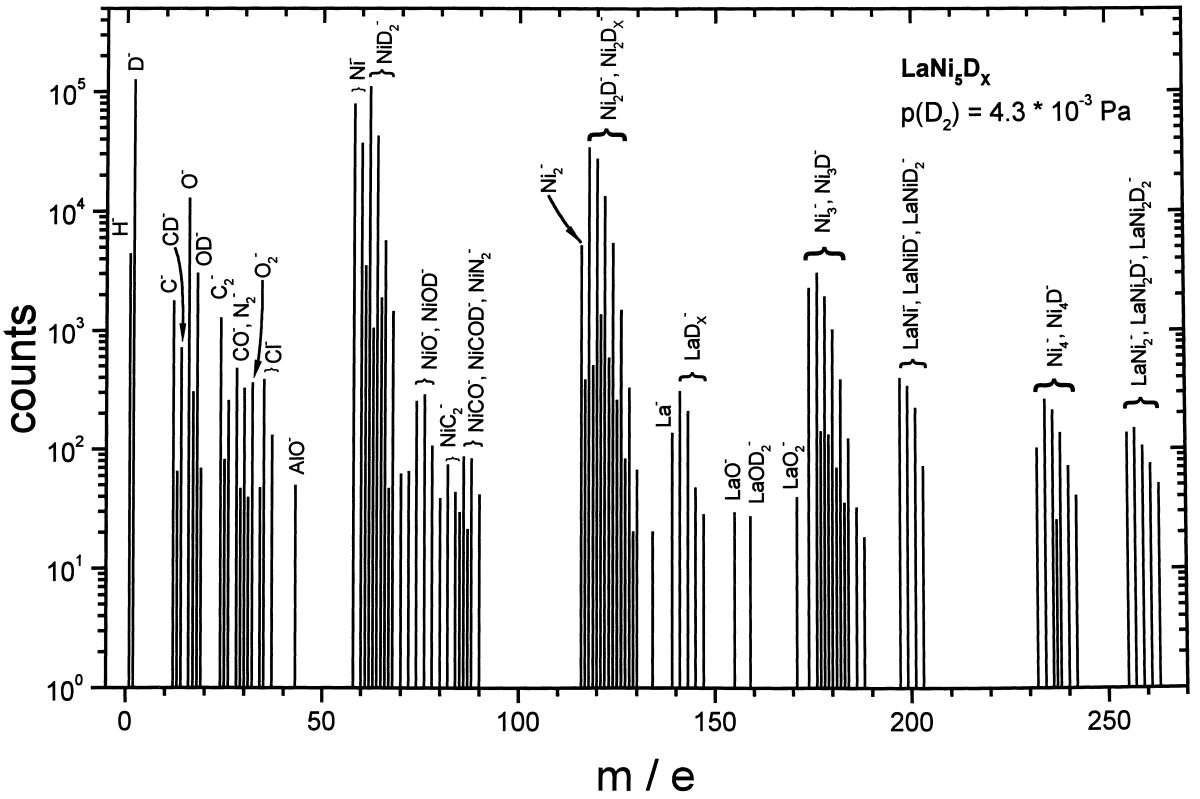

Fig. 4. Negative secondary ion mass spectrum of a $LaNi_5$ single crystal charged in situ with D_2.

$I(LaNi^+)=0.17$)[4] pointing to a rather weak lanthanum–deuterium bond in the sample.

The negative secondary ion mass spectrum of the $LaNi_5D_X$ sample (Fig. 4) is characterized by high absolute intensities of the deuterium containing cluster ions NiD_2^-, Ni_2D^-, NiD^-, $Ni_2D_2^-$ and $Ni_2D_3^-$. The cluster ions NiD_2^- and Ni_2D^- contain 90% of all metal bound deuterium atoms. Obviously these nickel–deuterium cluster ions, whose intensities exceed those of the corresponding deuterium free nickel ions (e.g. $I(Ni_2D^-)/I(Ni_2^-)\approx 6$), are preformed in the sample with a negative partial charge. This indicates a strong nickel–deuterium bond in the $LaNi_5D_X$ sample.

Since the total spectral intensity of the negative mass spectrum exceeds that of the positive mass spectrum by two orders of magnitude, the number of metal bound deuterium atoms is determined mainly by the negative spectrum. The deuterium content of the spectra $n(D_{metal})/n(M)\approx 0.9$ – that is the number of metal bound D atoms divided by the number of metal atoms – points to a high deuterium concentration of the sample.

The SIMS emission behavior of the in situ deuterium charged $LaNi_5$ is similar to that of an electrochemically charged sample (see [13]). This means the emission behavior does not depend on the applied charging technique. The advantages of the deuterium charging method applied here are improvements in spectral resolution and general performance. Since the deuterium concentration in the electrochemically charged sample corresponds to the β-hydride phase it can be concluded from the results on the $LaNi_5$ sample charged in situ by deuterium, that the observed spectrum is also representative of the β-hydride phase, though the deuterium charging pressure ($4.3\cdot10^{-3}$ Pa) is by orders of magnitude smaller than the bulk plateau pressure ($1.7\cdot10^5$ Pa) of the $LaNi_5$ hydrogen system. This extreme difference can be explained by a drastically enhanced deuterium solubility in the surface area distorted by the Ar^+ bombardment (see below and [1]).

3.1.2.2. $LaNi_{5-Y}Me_YD_X$ systems

Concerning the metal–deuterium cluster ions the secondary ion mass spectra of the $LaNi_{4.15}Al_{0.85}D_X$ sample (see the negative spectrum in Fig. 5) are very similar to the spectra of the deuterium charged $LaNi_5$ single crystal. No aluminum–deuterium cluster ions appear. Only the deuterium content of the spectra is slightly decreased due to the reduced number of nickel atoms available for the bond with deuterium. Nickel atoms are partially replaced by aluminum, which does not bind any deuterium in the ternary alloy. This explains the strong reduction in the

[4] As nickel is not an isotopically pure element the intensities of nickel containing deuterium cluster ions cannot be taken directly from the bar spectra but have to be calculated with the known natural abundance of nickel isotopes and the corresponding isotope patterns of ions containing more than one nickel atom.

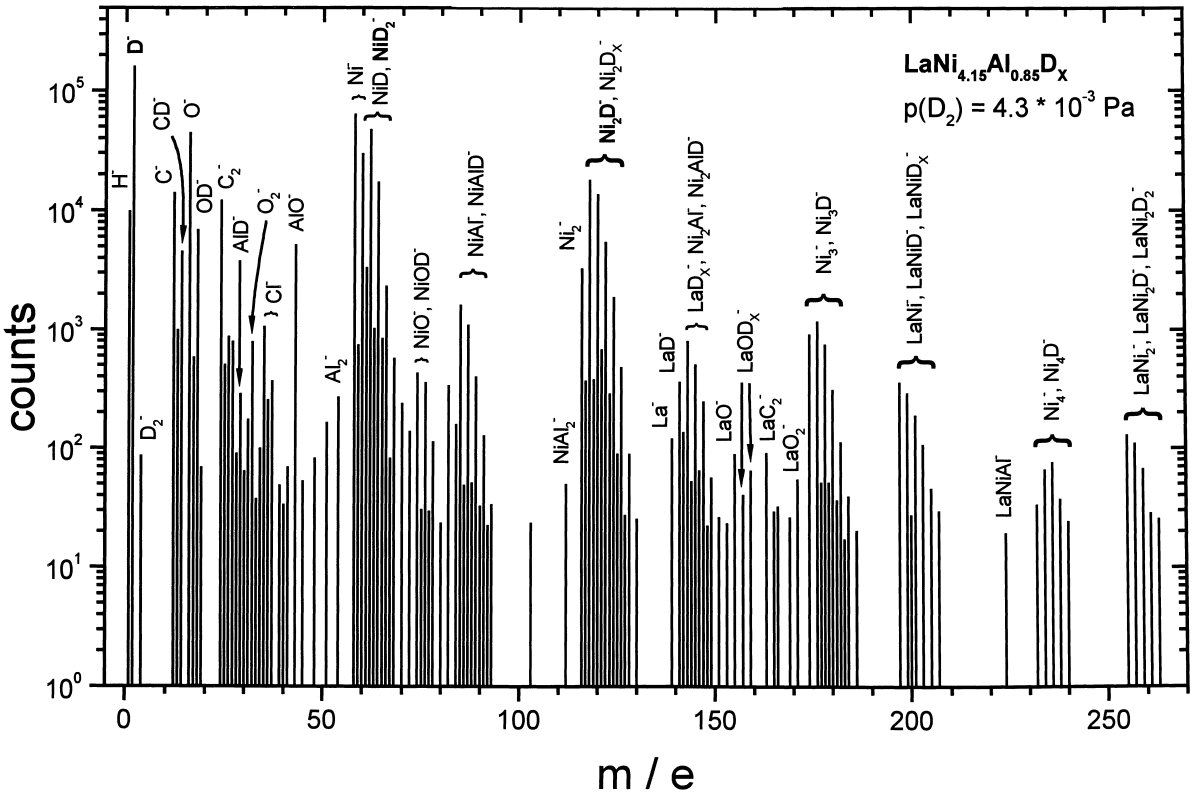

Fig. 5. Negative secondary ion mass spectrum of $LaNi_{4.15}Al_{0.85}$ charged in situ with D_2.

hydrogen storage capacity of the $LaNi_{5-X}Al_X$ compounds, known as the ''aluminum anomaly'' [14].

If silver is used as a nickel substituent AgD_2^- peaks appear in the negative secondary ion mass spectrum of $LaNi_{4.5}Ag_{0.5}D_X$ (see Fig. 6), pointing to a silver–deuterium bond in the alloy. As the intensity ratio $I(AgD_2^-)/I(Ag^-)$ is smaller than the comparable $I(NiD_2^-)/I(Ni^-)$ ratio the silver–deuterium bond seems to be weaker than the nickel–deuterium bond. This is the reason for the relatively small reduction in hydrogen storage capacity when nickel in $LaNi_5$ is substituted by silver.

The hydrogen bonding characteristics of the pure elements change drastically in the AB_5-type alloys. Nickel and silver become ''hydride formers'' and lanthanum and aluminum lose their hydrogen bonding properties in the alloys.

In an additional experiment the secondary ion intensity ratio $I(Ni_2D^-)/I(Ni_2^-)$, which serves as a measure of the deuterium concentration of the samples, has been measured for different $LaNi_{5-X}Al_X$ ($X=0$, 0.7, 0.85) alloys[5] as a function of the in situ deuterium charging pressure during the SIMS experiment. As the maximum deuterium pressure is far below the bulk plateau pressures of the hydrogen storage compounds studied here a Sieverts plot [15] has been chosen for graphical presentation (see Fig. 7) of the pressure concentration like ''SIMS isotherms''.

Instead of the expected linear Sieverts behavior the isotherms for all samples pass through a flat plateau-like region for deuterium pressures below 10^{-4} Pa. At higher pressures the isotherms rise in the diagram approaching a saturation intensity ratio $I(Ni_2D^-)/I(Ni_2^-)$, which is no longer influenced by a further increase in pressure. The shape of the ''SIMS isotherms'' is roughly comparable with the shape of bulk pressure–concentration diagrams in the two phase region (plateau) and the β-hydride phase of simple metal hydrogen systems. At high deuterium pressures ($>4\cdot10^{-4}$ Pa) the saturation intensity ratio decreases with increasing aluminum concentration of the samples. This behavior is in qualitative agreement with the bulk behavior of the samples and shows a decreasing hydrogen storage capacity with increasing Al-concentration. Besides the absence of aluminum–deuterium cluster ions in the secondary ion mass spectra (see above) this is an additional hint that aluminum and deuterium do not interact in $LaNi_{5-X}Al_XD_Y$.

In former investigations [1,16–18] it was reported that Ar^+ bombardment during SIMS analysis induces a hydrogen surface enrichment in metal hydrogen systems. However, even for the vanadium hydrogen system (plateau pressure $\approx10^{-3}$ Pa) a two phase region similar to that shown in Fig. 7 had not been observed in analogous

[5] Measurements were performed at reduced primary ion current densities of $4\cdot10^{-7}$ A/cm^2 in order to minimize the influence of the primary ion current density on the secondary ion emission [19].

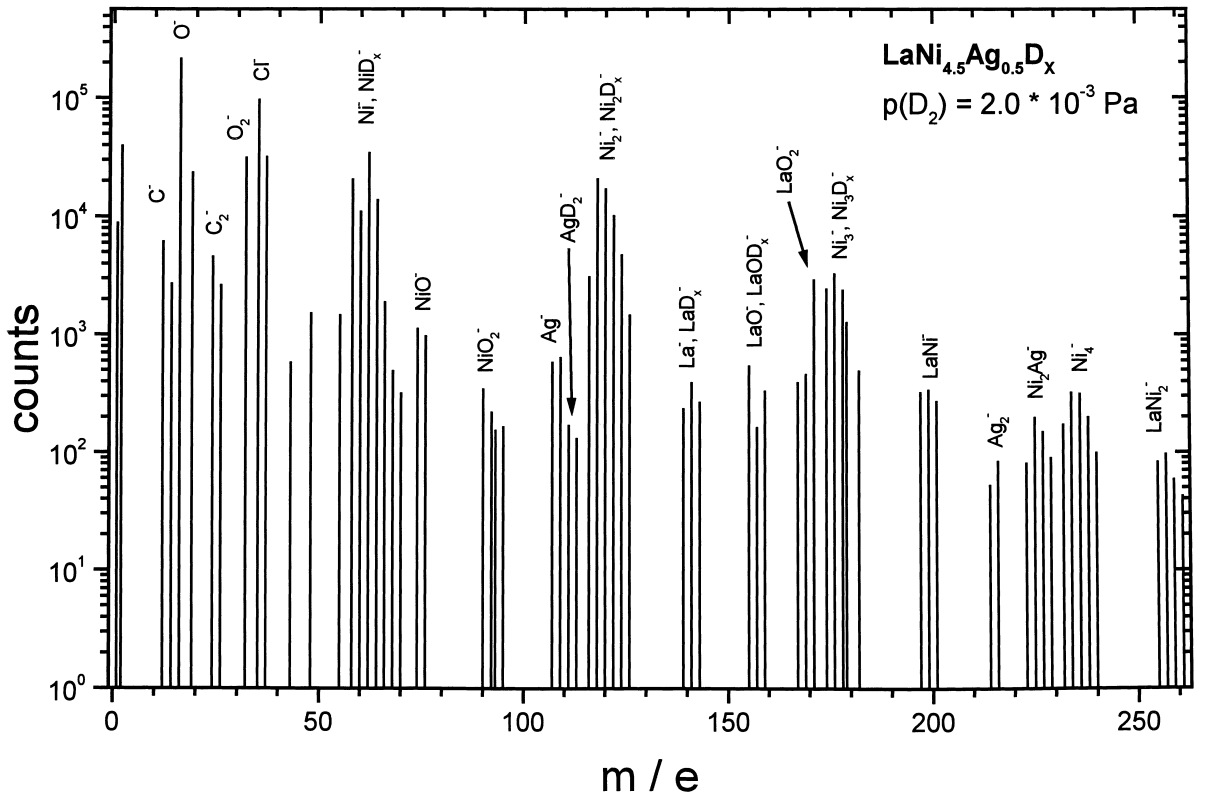

Fig. 6. Negative secondary ion mass spectrum of $LaNi_{4.5}Ag_{0.5}$ charged in situ with D_2.

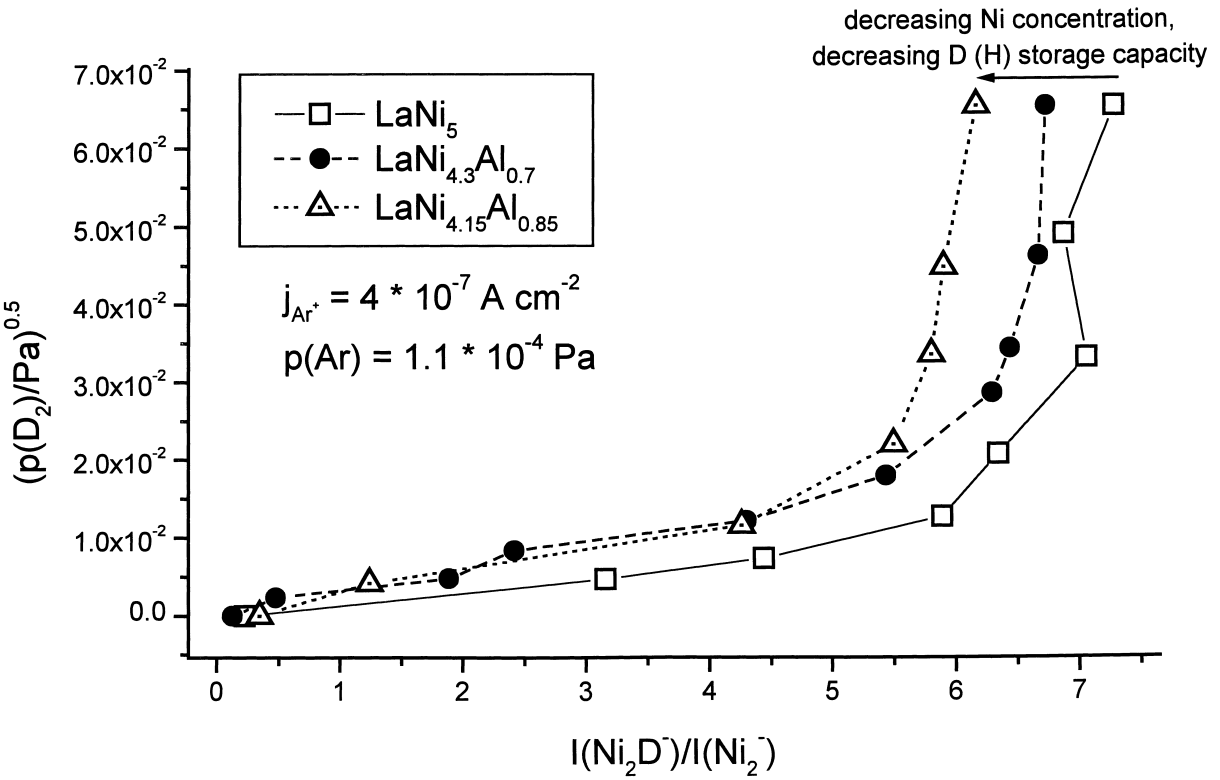

Fig. 7. Sieverts plot of secondary ion intensity ratios $I(Ni_2D^-)/I(Ni_2^-)$.

''SIMS isotherms''. The main reason for the absence of a real two phase region in the V–H system is the limitation of the maximum hydrogen concentration in the surface area by the applied high primary ion current [16,17] and by the hydrogen diffusion from the bulk to the surface region [18]. The limited hydrogen concentration results from the experimental conditions: the vanadium was charged gas-volumetrically *before* SIMS analysis and not in situ *during* SIMS analysis.

The clear differences in the plateau pressures of the bulk $LaNi_{5-X}Al_X$ compounds are not observable in the ''SIMS isotherms''. If the known plateau pressures of the bulk alloys [20] are extrapolated in a log p–$V_{unit\ cell}$-diagram (see Fig. 8) to plateau pressures obtained by SIMS analysis ($\approx 5\cdot 10^{-5}$ Pa), the effect of strongly reduced and equalized plateau pressures can be explained by an expansion of the unit cell caused by the Ar^+ bombardment. Furthermore, the expansion of the crystal lattice by the in situ deuterium charging could be detected by a visible deformation and cracking in the SIMS analysis spot [19], after demounting the samples from the SIMS instrument.

The lattice expansion to a volume of about 100 $Å^3$ corresponds quite well to the transition from the α- to the β-phase of $LaNi_5H_X$. This means, the lattice distortion caused by the Ar^+-ion bombardment produces a surface phase comparable with regard to hydrogen solubility to the β-phase of the alloy hydrogen system.

3.2. XPS

The $LaNi_5$ single crystal was cleaned by Ar^+ sputtering until no oxygen, carbon and nitrogen could be detected in a survey photoelectron spectrum. Hydrogen charging has been done by ion implantation (8 keV, dose=$2\cdot 10^{18}$ H atoms/cm^2) immediately after sputtering. The ion beam consists mainly of H_2^+ (91% H_2^+, 4.5% H^+, 4.5% H_3^+ [21]).

H_2^+ ion implantation without sample cooling led to photoelectron spectra identical to the Ar^+ sputtered, uncharged $LaNi_5$ [19]. That means that the sample is completely discharged within the short period of about 5 min after finishing the implantation and starting the XPS experiment. It is known from thermal desorption spectra [22] that no hydrogen escapes from $LaNi_5H_{6.7}$ below a temperature of 160 K. Therefore, the sample holder has been cooled with liquid nitrogen during the ion implantation and the XPS measurements. To avoid surface re-contamination by gases such as oxygen and hydrocarbons photoelectron spectra were acquired within 15 min after finishing ion implantation.

The valence band (Fig. 9) is shifted by 0.2 eV to higher binding energies in the hydrogen charged state. A hydrogen induced band appears at E_B=8–9 eV and the valence band width is reduced by 0.15 eV. These experimental results are in agreement with band structure calculations

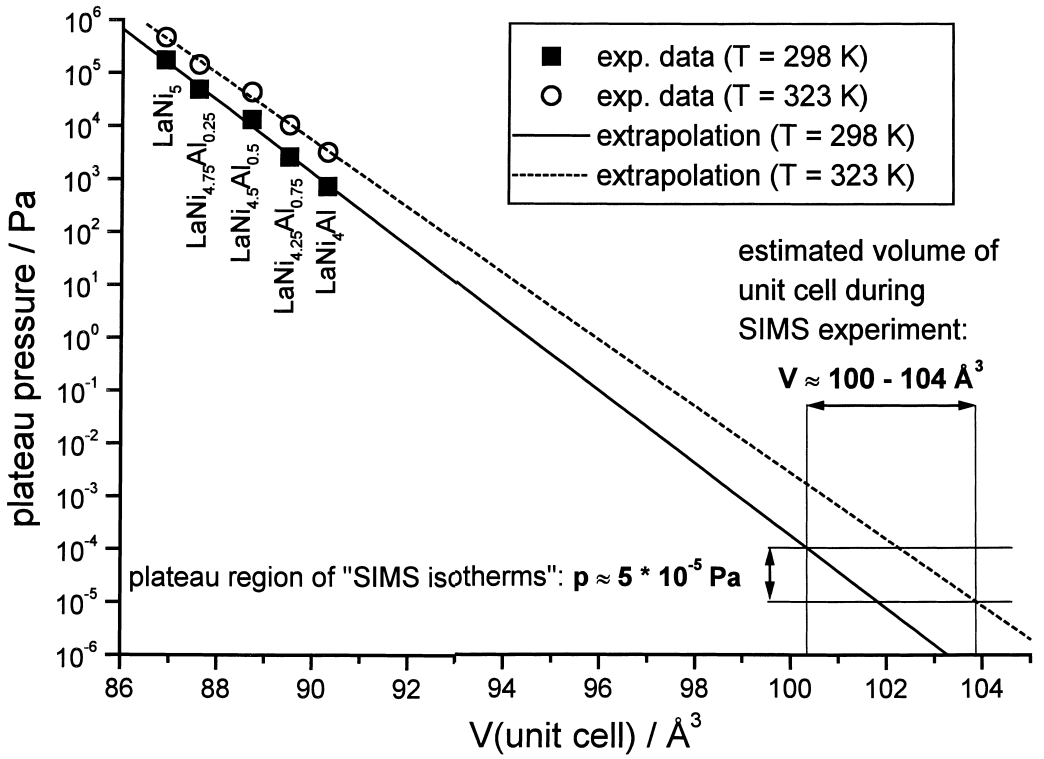

Fig. 8. Plateau pressure–volume of unit cell diagram, data after [20].

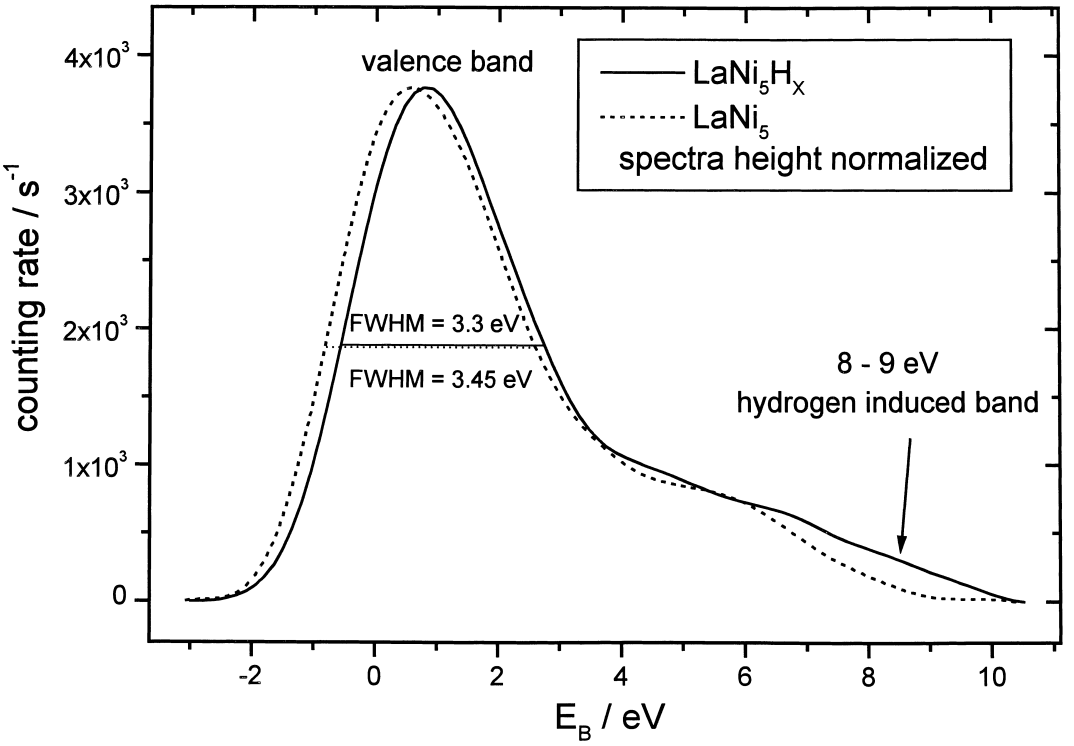

Fig. 9. XPS valence band spectra of a H_2^+ implanted and an uncharged $LaNi_5$ single crystal.

[23]: as the Fermi energy E_F serves as the reference level in photoelectron spectroscopy the calculated shift of the Fermi energy corresponds with the XPS valence band shift. Due to the hydrogen charging the energy density of states is reduced at E_F.

The hydrogen induced chemical shift of the La 3d and Ni 2p core levels (Fig. 10) can be determined with the highest accuracy by the energy difference ΔE_B(Ni $2p_{1/2}$ − La $3d_{5/2}$)=33.45 eV, which is reduced by 0.15 eV compared to uncharged $LaNi_5$. In the electrostatic charge potential model this can be explained by a more negatively charged nickel in $LaNi_5H_X$ than in $LaNi_5$. This fact points to a Ni–H bond in the alloy. The effect of atomic renormalization [24] is another explanation of the chemical shift: according to SIMS experiments and to the band structure calculation [23] hydrogen is bound preferably to nickel in $LaNi_5H_X$. An increased valence electron density between the nickel and hydrogen sites together with a reduced atomic volume of nickel in the hydrogen charged $LaNi_5$ results in an electrostatic repulsion of the valence electrons and nickel core electrons, leading to reduced binding energies of the nickel core levels.

The intensity of the nickel *shake-up* satellite corresponds with the number of unfilled energy levels having nickel 3d character and depends on the energy difference between these levels and the Fermi level [25]. The reduced Ni $2p_{1/2}$ *shake-up* intensity in $LaNi_5H_X$ compared to that in $LaNi_5$ (Fig. 11) indicates, therefore, a partial filling of the Ni 3d electron holes by the electrons of the H atoms. This result is in agreement with band structure calculations [23]. An additional line shape effect occurs at the La $3d_{5/2}$ line (Fig. 12): the well screened $3d^9 4f^1$ intensity is reduced by hydrogen charging because the density of filled electron states at the Fermi level is reduced and the probability for an electron transfer from the valence band into the 4f state is decreased.

4. Conclusions

SIMS and XPS measurements are both excellent methods for examining the bonding properties of metal hydrogen systems if skillful sample preparation and special experimental conditions are applied. An advantage of SIMS compared to XPS is that hydrogen can be detected directly even in the presence of contaminations. However, the SIMS results obtained with in situ prepared, clean surfaces contain more information than those obtained with contaminated samples. The advantage of XPS results stems from the fact that they can be compared directly with theoretical hydrogen bonding models and that their analysis is more straightforward.

The enhanced hydrogen solubility induced by ion sputtering allows a SIMS analysis even of metal hydrogen

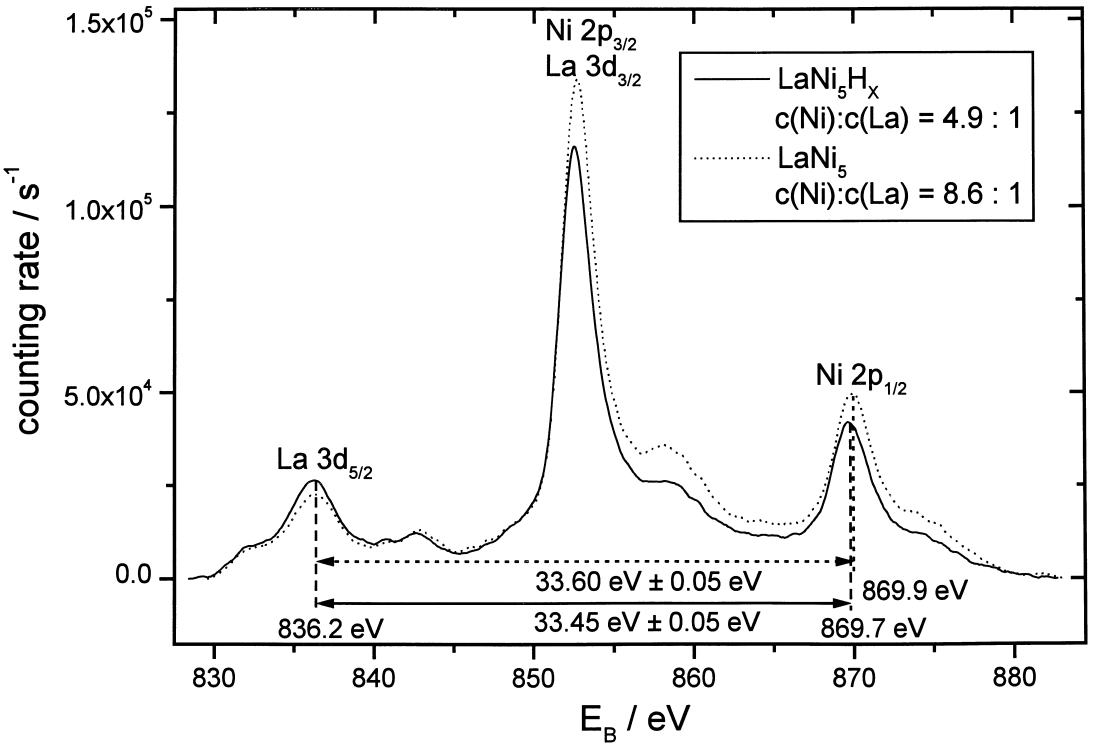

Fig. 10. XPS La 3d and Ni 2p core level spectra of a H_2^+ implanted and an uncharged $LaNi_5$ single crystal.

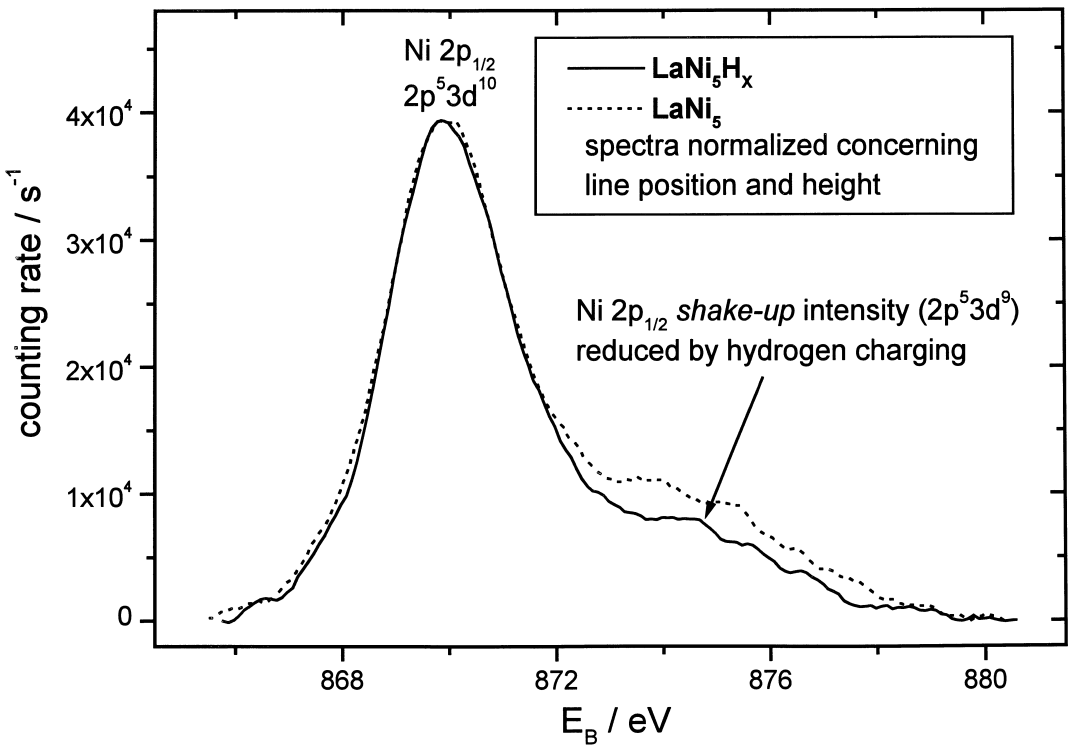

Fig. 11. XPS Ni $2p_{1/2}$ core level spectra of a H_2^+ implanted and an uncharged $LaNi_5$ single crystal.

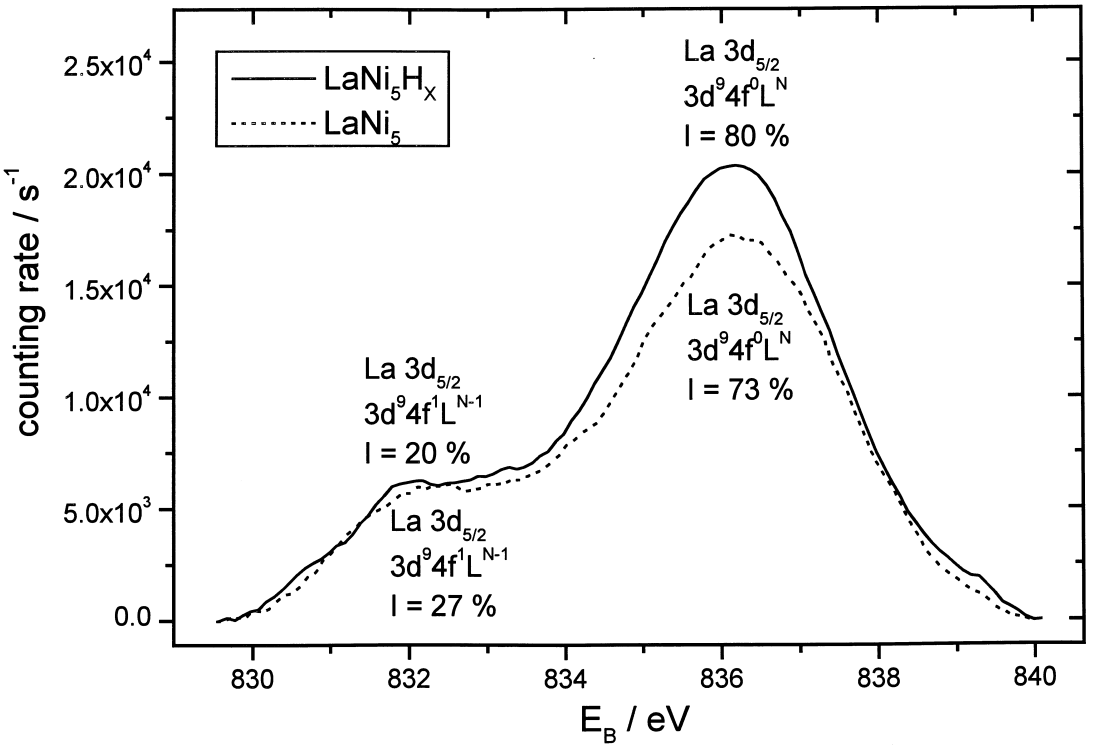

Fig. 12. XPS La $3d_{5/2}$ core level spectra of a H_2^+ implanted and an uncharged $LaNi_5$ single crystal.

systems, which are expected to be unstable under the vacuum conditions required. The SIMS results are generally characteristic of the high hydrogen concentration phase of the samples. Nevertheless, differences in hydrogen storage capacity depending on the alloy composition are observable with reliability.

In cases where in situ gasvolumetric hydrogen charging is not sufficient to see hydrogen induced changes in the SIMS and XPS spectra H_2^+ ion implantation can be applied. The XPS results on $LaNi_5H_X$ support the theoretical results obtained from band structure calculations.

References

[1] J. Scholz, H. Züchner, H. Paulus, K.-H. Müller, J. Alloys Comp. 253–254 (1997) 459.
[2] T. Riesterer, Z. Phys. B. Condensed Matter 66 (1987) 441.
[3] H.C. Siegmann, L. Schlapbach, C.R. Brundle, Phys. Rev. Lett. 40 (1978) 972.
[4] D.X. Zhang, X.L. Wang, G.S. Wang, Z. Physik. Chem. N.F. 164 (1989) 1441.
[5] P. Selvam, B. Viswanathan, C.S. Swamy, V. Srinivasan, Z. Physik. Chem. N.F. 164 (1989) 1199.
[6] X.-L. Wang, S. Suda, J. Alloys Comp. 194 (1993) 73.
[7] N. Kuriyama, T. Sakai, H. Miyamura, H. Tanaka, I. Uehara, F. Meli, L. Schlapbach, J. Alloys Comp. 238 (1996) 128.
[8] H. Züchner, P. Kock, Z. Physik. Chem. N.F. 164 (1989) 1165.
[9] J. Kintrup, H. Züchner, Z. Naturforsch 50a (1995) 381.
[10] M.P. Seah, Surf. Interf. Anal. 14 (1989) 488.
[11] D.A. Shirley, Phys. Rev. B 5 (1972) 4709.
[12] R. Dobrileit, Thesis, Münster, 1998
[13] H. Züchner, R. Dobrileit, T. Rauf, Fresenius J. Anal. Chem. 341 (1991) 219.
[14] K.A. Gschneidner Jr., T. Takeshita, Y. Chung, O.D. McMasters, J. Phys. F: Met. Phys. 12 (1982) L1.
[15] A. Sieverts, Z. Physik. Chem. 88 (1914) 451.
[16] H. Züchner, B. Hüser, Z. Physik. Chem. N.F. 147 (1986) 35.
[17] H. Züchner, B. Hüser, P. Kock, Fresenius Z. Anal. Chem. 329 (1987) 169.
[18] H. Züchner, P. Kock, T. Brüning, T. Rauf, R. Dobrileit, J. Less-Common Met. 172–174 (1991) 95.
[19] J. Kintrup, Thesis, Münster, 1998
[20] H. Diaz, A. Percheron-Guégan, J.C. Achard, C. Chatillon, J.C. Mathieu, Int. J. Hydrogen Energy 4 (1979) 445.
[21] Y. Baba, T.A. Sasaki, J. Nucl. Mater. 138 (1986) 149.
[22] A. Resnik, M. Stioui, A. Grayevsky, D. Shaltiel, J. Less-Common Met. 131 (1987) 117.
[23] M. Gupta, J. Less-Common Met. 130 (1987) 219.
[24] W.F. Egelhoff, Surf. Sci. Rep. 6 (1987) 253.
[25] F.U. Hillebrecht, J.C. Fuggle, P.A. Bennett, Z. Zolnierek, C. Freiburg, Phys. Rev. B 27 (1983) 2179.